

Studies of the reactivity of artificial peroxidase-like hemoproteins based on antibodies elicited against a specifically designed *ortho*-carboxy substituted tetraarylporphyrin

Solange de Lauzon, Bernard Desfosses, Daniel Mansuy, Jean-Pierre Mahy*

Laboratoire de Chimie et Biochimie Pharmacologiques et Toxicologiques, URA 400 CNRS, Université Paris V, 45 Rue des Saints-Pères, 75270 Paris Cedex 06, France

Received 23 October 1998; received in revised form 14 December 1998

Abstract The temperature and pH dependence as well as the selectivity of the peroxidase activity of a complex associating a monoclonal antibody 13G10 with its iron(III)- $\alpha,\alpha,\alpha,\beta$ -*meso-tetrakis(ortho-carboxyphenyl)* porphyrin (Fe(ToCPP)) hapten have been studied and compared to those of Fe(ToCPP) alone. It first appears that the peroxidase activity of the 13G10-Fe(ToCPP) complex is remarkably thermostable and remains about 5 times higher than that of Fe(ToCPP) alone until at least 80°C. Secondly, this complex is able to use not only H₂O₂ as oxidant but also a wide range of hydroperoxides such as alkyl, aralkyl and fatty acid hydroperoxides and catalyze their reduction 2–6-fold faster than Fe(ToCPP) alone. It is also able to catalyze the oxidation by H₂O₂ of a variety of reducing cosubstrates such as 2,2'-azinobis(3-ethylbenzothiazoline-6-sulfonic acid) (ABTS), *o*-phenylenediamine (OPD), 3,3',5,5'-tetramethylbenzidine (TMB) and 3,3'-dimethoxybenzidine 3–8-fold faster than Fe(ToCPP) alone, the bicyclic aromatic ABTS and TMB being the best reducing cosubstrates. Finally, a pH dependence study, between pH 4.6 and 7.5, of the oxidation of ABTS by H₂O₂ in the presence of either 13G10-Fe(ToCPP) or Fe(ToCPP) shows that $K_m(\text{H}_2\text{O}_2)$ values vary very similarly for both catalysts, whereas very different variations are found for the k_{cat} values. With Fe(ToCPP) as catalyst the k_{cat} value remains constant around 100 min⁻¹ whereas with the 13G10-Fe(ToCPP) complex, it increases sharply below pH 5 to reach 540 min⁻¹ at pH 4.6. This could be due to the participation of a carboxylic acid side chain of the antibody protein, as a general acid-base catalyst, to the heterolytic cleavage of the O–O bond of H₂O₂ leading to the highly reactive iron(V)-oxo intermediate in the peroxidase mechanism. Accordingly, the modification of the carboxylic acid residues of antibody 13G10 by glycnamide leads to a 50% decrease of the peroxidase activity of the 13G10-Fe(ToCPP) complex.

© 1999 Federation of European Biochemical Societies.

Key words: Catalytic antibody; Peroxidase; Artificial hemoprotein; Porphyrin

1. Introduction

Most of the catalytic antibodies reported to date [1–5] have been obtained by producing monoclonal antibodies that have been elicited against transition state analogs. In those cases, only the antibody protein, through some amino acid residues of its binding site, is fully responsible for catalysis. In some cases however, monoclonal antibodies require the presence of

a cofactor, such as inorganic cofactors [6,7] or natural cofactors like flavins [8], metal ions [9–12] or metal complexes [13–26], to be catalytic. The antibody protein then binds the cofactor tightly and enhances its reactivity and/or provides a template which controls the positioning of the substrate with respect to the cofactor and influences the selectivity of the reaction. Accordingly, the association of antibodies with metalloporphyrin cofactors represented a promising route to model systems for hemoproteins such as peroxidases [27] and cytochromes P450 [28]. Therefore, antibodies have been elicited against *meso*-carboxy-aryl-substituted [14,18,23,26,29], *N*-substituted [15,16,22,24,25] and Sn- [17,19] or Pd-porphyrins [20,21]. Four of the antibodies obtained [16,22,23,29] have shown, in the presence of the corresponding iron(III)-porphyrin cofactor, a significant peroxidase activity characterized by k_{cat}/K_m values ranging between 10² and 5 × 10³ M⁻¹ s⁻¹. Only one of the antibodies was reported to exhibit, in the presence of Mn(III)-*tetrakis(para-carboxyvinylphenyl)*porphyrin, a weak monooxygenase-like activity [17]. We recently reported the production of monoclonal antibodies elicited against iron(III)- $\alpha,\alpha,\alpha,\beta$ -*meso-tetrakis(ortho-carboxyphenyl)* porphyrin (Fe(ToCPP)) **1**, 13G10 and 14H7, which were not only able to bind the hapten with K_d values of about 10⁻⁹ M, but also exhibited, in the presence of Fe(ToCPP), a significant peroxidase activity characterized by k_{cat}/K_m values of about 10² M⁻¹ s⁻¹ [29]. An active site topology was further proposed for these antibodies on the basis of comparative studies of the dissociation constants of various porphyrin-antibody complexes as well as amino acid sequences of L and H chains and chemical modifications of amino acid side chains of the antibody protein [30]. It thus appeared that roughly two thirds of the porphyrin macrocycle were inserted in the binding pocket, with three of the *ortho*-carboxylate substituents of the *meso*-phenyl rings of the porphyrin being recognized by amino acid side chains of the antibody, whereas no amino acid residue was coordinating the central iron atom. In addition, arginine residues appeared to be involved in the recognition of those carboxylates, but they did not seem to participate in catalysis.

We here report kinetic studies of the peroxidase reactions catalyzed by the 13G10-**1** complex, compared to those catalyzed by **1** alone. The results obtained show that: (i) the peroxidase activity of the IgG-**1** complex is highly thermostable and remains about five times higher than that of **1** alone until at least 80°C. (ii) The 13G10-**1** complex is able to catalyze the reduction not only of hydrogen peroxide but also of alkyl and aralkyl hydroperoxides as well as the oxidation of a wide range of reducing cosubstrates by H₂O₂ with a 2–8-fold higher efficiency than **1** alone. (iii) A pH dependence study of the

*Corresponding author. Fax: (33) 1 42 86 83 87.
E-mail: mahy@bisance.citi2.fr

oxidation of 2,2'-azinobis(3-ethylbenzothiazoline-6-sulfonic acid) (ABTS) by H_2O_2 , in the presence of either **1** alone or its complex with 13G10, shows that the rate acceleration by the antibody-**1** complex could be due to the participation of a carboxylate residue from the protein in the catalysis of the heterolytic cleavage of the O-O bond of H_2O_2 .

2. Materials and methods

2.1. Synthesis of Fe(ToCPP) **1**

The four atropoisomers of *meso-tetrakis(ortho-carboxymethylphenyl)* porphyrin (ToCMePPH₂) were first synthesized and separated on a silica gel column as described previously by Leondiadis and Momen-teau [31]. The $\alpha,\alpha,\alpha,\beta$ isomer was separated with CH_2Cl_2 -Et₂O 80/20 (v/v) as eluent ($R_f = 0.4$) and was identified by its UV-visible and ¹H NMR spectra which were found to be identical to those already described [31]. $\alpha,\alpha,\alpha,\beta$ -Fe(ToCMePP) was then prepared according to a previously described procedure [32], by reaction of $\alpha,\alpha,\alpha,\beta$ -ToCMePPH₂ with $\text{Fe}(\text{CO})_5$ in the presence of I_2 in toluene at room temperature to avoid isomerization. $\alpha,\alpha,\alpha,\beta$ -Fe(ToCPP) **1** was subsequently obtained by saponification of the *ortho*-methyl ester substituents in 2 N KOH in 80% EtOH at room temperature [31]. The obtained iron(III)-porphyrin was characterized by UV-visible (λ_{max} (nm), ϵ (mM⁻¹) in DMSO = 422 (81), 534 (11), 693 (3.1)) and mass (MALDI-TOF; $m/z = 900.8$ (100%, $\text{M} + \text{Na}^+$)) spectroscopies.

2.2. Preparation of monoclonal antibodies

Monoclonal antibodies were generated as reported in a previous paper [30]. Briefly, **1** was activated by *N*-hydroxysuccinimide and covalently attached to KLH (keyhole limpet hemocyanin) and to BSA (bovine serum albumin) in phosphate buffered saline pH 7.5. The conjugates were then purified by column chromatography on Biogel P10. Hapten-carrier protein ratios determined spectrophotometrically were in the range of 15/1 to 20/1. Four five-week-old, female BALB/c mice were immunized by intraperitoneal injection of 400 μl of an emulsion of the hapten-KLH conjugate (75 μg) in complete Freund's adjuvant. Two other immunizations were done 2 weeks and 5 weeks later with 75 μg hapten-KLH emulsified in incomplete Freund's adjuvant. The mouse showing the best immune response 12 days after the third immunization was boosted both intravenously and intraperitoneally with 75 μg hapten-KLH in saline solution and was killed 3 days later. Its splenocytes were fused with PAI myeloma cells according to Köhler and Milstein [33]. The resulting hybridomas were screened by ELISA for binding to the hapten-BSA conjugate using peroxidase-linked goat anti-mouse antibodies [34]. Positive hybridomas were cloned twice and propagated in ascites. Antibodies were then purified on a column of protein A and their homogeneity and purity were checked by SDS gel electrophoresis.

2.3. Assay of peroxidase activity

All the reducing cosubstrates used in this study: ABTS diammonium salt, 98%, 3,3'-dimethoxybenzidine (DMB) dihydrochloride purified, OPD dihydrochloride, 3,3',5,5'-tetramethylbenzidine (TMB) dihydrochloride and pyrogallol ACS reagent, were from Sigma. Hydrogen peroxide 30% in water was from Prolabo, *tert*-butylhydroperoxide 70% in water was from Janssen and cumylhydroperoxide 80% in cumene was from Merck. Fatty acid hydroperoxides, 15(*S*)-

hydroperoxy-eicosatetraenoic acid (15-HPETE) and 13(*S*)-hydroperoxy-octadecatrienoic acid (13-HPOD) (95%) were from Sigma.

All reactions were carried out in the presence of either 0.2 μM **1** alone or 0.2 μM **1** and 0.5 μM 13G10 as catalysts.

Furthermore, for the temperature dependence studies, the oxidation of 0.2 mM ABTS by 0.7 mM H_2O_2 was performed between 5 and 80°C in 0.1 M acetate buffer, pH 4.6, containing 0.2% DMSO. The absorbance was monitored at 414 nm using an UVIKON 860 UV-visible spectrometer. The initial rates of oxidation were determined from the slope at the origin of the curve representing the variations of the absorbance at 414 nm as a function of time using an ϵ value of 28 000 $\text{M}^{-1} \text{cm}^{-1}$.

The reactions of various oxidants (H_2O_2 , ethyl-, *tert*-butyl- and cumylhydroperoxide), 0.7 mM, with 0.2 mM ABTS and the reactions of 0.7 mM H_2O_2 with respectively ABTS, DMB, OPD, TMB and pyrogallol, 0.2 mM were performed at 20°C in 0.1 M citrate-0.05 M phosphate buffer, pH 5.0. The absorbance was monitored respectively at 414, 465, 450, 650 and 420 nm using an UVIKON 860 UV-visible spectrometer. The initial rates of oxidation were determined from the slope at the origin of the curve representing the variations of the absorbance at respectively 414, 465, 450, 650 and 420 nm using respectively ϵ values of 28 000, 21 800, 10 500, 13 600 and 1800 $\text{M}^{-1} \text{cm}^{-1}$.

For the pH dependence studies, H_2O_2 at concentrations varying between 40 μM and 30 mM was incubated at 20°C with ABTS, at concentrations varying between 10 μM and 10 mM, in 0.1 M citrate-0.05 M phosphate buffer, pH 4.6, 5, 6, 7 and 7.5, and Lineweaver-Burk plots were established in each case.

2.4. Chemical modification of 13G10

The carboxylate residues of the antibody protein were modified according to a previously described procedure [35]. In a typical experiment, a solution at pH 4.75 containing antibody 13G10 (20 μM), glycinamide (1 M) and 1-ethyl-3-dimethylaminopropylcarbodiimide (EDC) (0.4 M) was incubated for 1 h at 25°C. After a second addition of EDC (0.4 M), the reaction mixture was incubated for one more hour at 25°C. Throughout the experiment the pH was controlled and maintained at 4.75 with a pH-stat (665 Dosimat, Metrohm) by addition of 0.1 M HCl. The mixture was then dialyzed for 48 h against 20 mM phosphate buffer, pH 6. The peroxidase activity of the modified IgG-**1** complex was then determined as described above. To measure the protective effect of hapten **1** on this modification, the same reaction was carried out under similar conditions starting from 13G10 previously incubated 1.5 h at 20°C with 40 μM **1**.

3. Results

3.1. Thermostability of the peroxidase activity

The peroxidase activity of the 13G10-**1** complex was assayed at temperatures varying between 5 and 80°C and compared with that of **1** alone (Fig. 1). With both catalysts, the initial rate of oxidation of ABTS by H_2O_2 increased with the temperature to reach an approximately 10-fold higher value at 80°C than at 5°C. In addition, the rate of oxidation measured in the presence of 13G10-**1** as catalyst remained about 5-fold higher than that measured in the presence of **1** alone, even at 80°C. Thus, the IgG-**1** complex appeared to be a remarkably

Table 1
Oxidation of various reducing cosubstrates by H_2O_2 at pH 5, catalyzed by Fe(ToCPP) **1** and its complex with antibody 13G10^a

Catalyst	Rate of oxidation ^b (turnovers/min)			
	Reducing cosubstrate			
	ABTS	DMB	OPD	TMB
1	0.85 ± 0.08	0.26 ± 0.02	0.46 ± 0.04	1.26 ± 0.13
13G10- 1	4.72 ± 0.38	2.06 ± 0.20	1.54 ± 0.15	5.75 ± 0.46
13G10- 1 ^c	5.7 ± 0.9	7.9 ± 1.3	3.3 ± 0.6	4.5 ± 0.8

^aFor experimental conditions see Section 2.

^bThe turnover numbers presented here are net values obtained after subtraction of the rates of oxidation observed for the reactions performed without catalyst, which ranged between 6.2 and 16 nM oxidized cosubstrate/min.

^cRate enhancement observed after complexation of **1** to antibody 13G10.

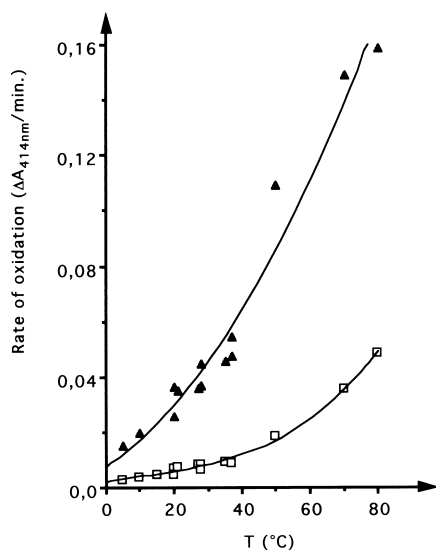


Fig. 1. Temperature dependence of the peroxidase activity. The rate of oxidation of 0.2 mM ABTS by 0.7 mM H_2O_2 in 0.1 M acetate buffer pH 4.6 was measured between 5 and 80°C in the presence of Fe(ToCPP) (□) or 13G10-Fe(ToCPP) (▲) as catalyst.

thermostable catalyst and remained more efficient than **1** alone even at 80°C.

3.2. Specificity of the peroxidase activity

The specificity of the peroxidase reaction was first examined using different reducing cosubstrates (ABTS, OPD, TMB, pyrogallol and DMB) in the presence of hydrogen peroxide as oxidant. The initial rates of oxidation in the presence of either **1** or 13G10-**1** as catalyst were calculated as described in Section 2, and the rate enhancement due to the binding of **1** to antibody 13G10 was evaluated by the ratio of those two rates. A preliminary pH dependence study for all those reducing cosubstrates (Fig. 2) showed that the rate enhancement increased when the pH decreased and was optimal at (DMB) or below pH 5. Further studies were thus undertaken at pH 5 and the corresponding values of the rates of oxidation as well as the rate enhancements are summarized in Table 1. Under those conditions, both **1** and 13G10-**1** catalyzed the oxidation of ABTS, OPD, TMB and DMB, whereas pyrogallol was not oxidized. The best rate enhancement, 7.9 ± 1.3 , was observed

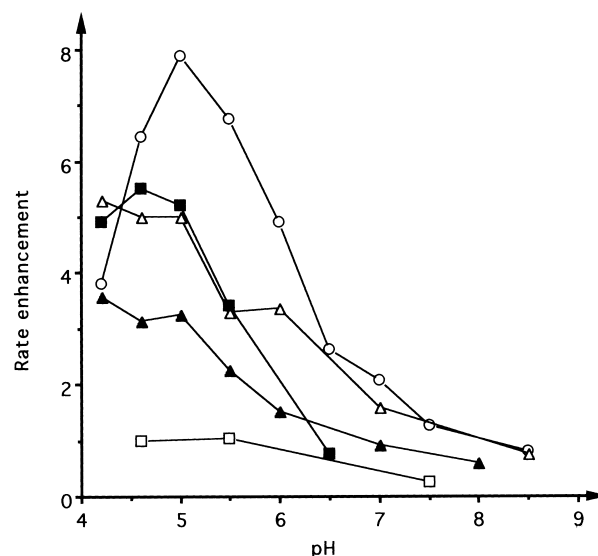


Fig. 2. pH dependence of the rate enhancement due to the binding of Fe(ToCPP) **1** to antibody 13G10 for the oxidation of various reducing cosubstrates: *o*-dianisidine (○), TMB (■), OPD (▲), pyrogallol (□) and ABTS (△), 0.2 mM by 0.7 mM H_2O_2 . The rate enhancement was determined as the ratio of the rate of oxidation measured with 13G10-**1** as catalyst over that measured with **1** alone as catalyst.

in the case of DMB while the highest rates of oxidation were observed in the case of ABTS (4.72 ± 0.38 turnovers/min) and TMB (5.75 ± 0.46 turnovers/min) using 13G10-**1** as catalyst. Since a better rate enhancement was found for ABTS (5.7 ± 0.9) than for TMB (4.5 ± 0.8 turnovers/min), the former compound was chosen as the reducing cosubstrate for all other kinetic studies described in this paper.

The oxidation of ABTS, in the presence of either **1** or 13G10-**1** as catalyst, was thus assayed using various hydroperoxides, including hydrogen peroxide, alkyl or aralkyl hydroperoxides or fatty acid hydroperoxides as oxidant. With the long chain hydrophobic fatty acid hydroperoxides 15-HPETE and 13-HPOD, the reaction was very fast with both catalysts (data not shown) and we were unable to determine accurately the rates of oxidation and the rate enhancement due to the binding of **1** to antibody 13G10. With other hydroperoxides, the reaction proceeded more slowly and those pa-

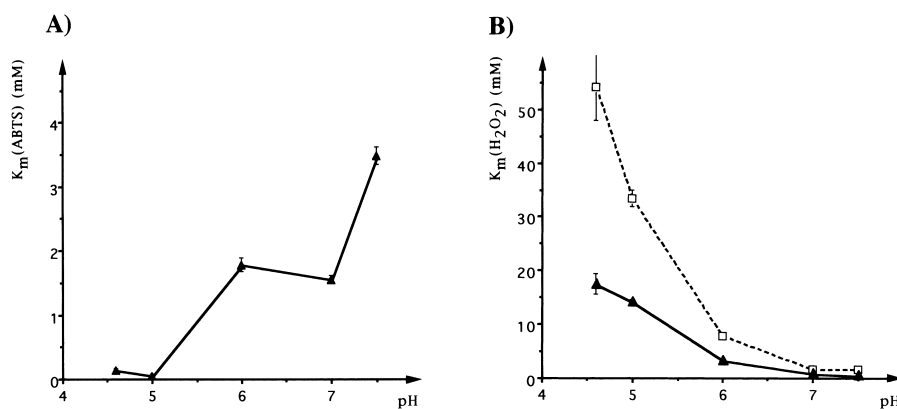


Fig. 3. pH dependence of the oxidation of ABTS (0.2 mM) by H_2O_2 (0.7 mM) in the presence of either **1** (□) or 13G10-**1** (▲) as catalyst. A: Variations of K_m (ABTS) as a function of pH. B: Variations of K_m (H_2O_2) as a function of pH. For experimental conditions see Section 2.

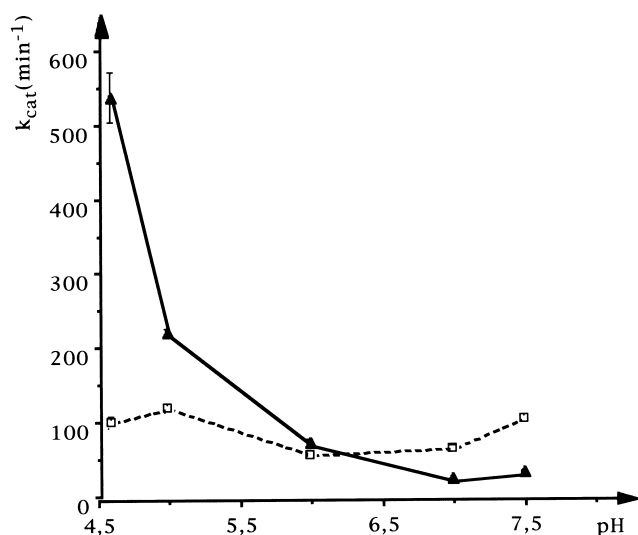


Fig. 4. pH dependence of the oxidation of ABTS (0.2 mM) by H₂O₂ (0.7 mM) in the presence of either **1** (□) or 13G10-1 (▲) as catalyst. Variations of k_{cat} as a function of pH.

rameters could be measured (Table 2). In all cases the reaction was catalyzed both by **1** and 13G10-1, the latter IgG-1 complex being the best catalyst. Ethylhydroperoxide appeared to be a poor oxidant and low rates were observed both with **1** (0.11 ± 0.01 turnovers/min) and with 13G10-1 (0.28 ± 0.03 turnovers/min). Better rates were observed with hydrogen-, *tert*-butyl- and cumylhydroperoxide which led to rate values between 0.61 ± 0.07 and 0.94 ± 0.11 turnovers/min with **1** as catalyst and between 1.83 ± 0.18 and 4.72 ± 0.38 turnovers/min with 13G10-1 as catalyst. The best rate enhancement was obtained with H₂O₂ (5.7 ± 0.9) whereas *tert*-butyl- and cumylhydroperoxide led to rate enhancements of 3.4 ± 0.7 and 1.9 ± 0.4 , respectively.

3.3. pH dependence of the peroxidase activity

In order to interpret the enhancement of the rate of the peroxidase reaction observed after the binding of **1** to antibody 13G10, the kinetic parameters of the oxidation of ABTS by H₂O₂ with either **1** or 13G10-1 as catalyst were determined at pHs varying between 4.6 and 7.5. With **1** as catalyst, the initial rate of oxidation increased gradually as a function of the concentration of ABTS and the reaction did not display saturation kinetics with respect to ABTS. In contrast, the same reaction performed with 13G10-1 as catalyst showed saturation kinetics with respect to ABTS and $K_m(\text{ABTS})$ values could be determined from Lineweaver-Burk plots. As

shown in Fig. 3A, when the pH increased from 4.6 to 7.5, $K_m(\text{ABTS})$ increased from 0.14 ± 0.01 to 3.48 ± 0.14 mM. For both catalysts, Michaelis-Menten kinetics were observed with respect to H₂O₂ and very similar variations were observed for $K_m(\text{H}_2\text{O}_2)$ (Fig. 3B). Indeed, when the pH increased from 4.6 to 7.5, with **1** as catalyst, $K_m(\text{H}_2\text{O}_2)$ decreased from 54.1 ± 6.2 to 1.52 ± 0.13 mM whereas with 13G10-1 as catalyst, $K_m(\text{H}_2\text{O}_2)$ decreased from 17.5 ± 1.9 to 0.47 ± 0.02 mM. In contrast, the variations of the k_{cat} values appeared to be very different for both catalysts (Fig. 4). In the presence of **1** as catalyst, the k_{cat} value remained almost constant (around 100 min^{-1}) over this pH range whereas it increased sharply below pH 5 in the presence of 13G10-1 to reach $540 \pm 33.8 \text{ min}^{-1}$ at pH 4.6. Consequently, when k_{cat}/K_m values are plotted against the pH, it appears clearly that the curves representing the variations of $k_{\text{cat}}/K_m(\text{H}_2\text{O}_2)$ as a function of pH are very similar with both catalysts and show a sharp increase, by a factor 10, around pH 7 (Fig. 5A). In addition, the curve representing the variations of $k_{\text{cat}}/K_m(\text{ABTS})$ as a function of pH (Fig. 5B) shows that $k_{\text{cat}}/K_m(\text{ABTS})$ increases by a factor 400 at acidic pH to reach a value of $69\,000 \pm 3000 \text{ M}^{-1} \text{ s}^{-1}$ at pH 5.0 with 13G10-1 as catalyst.

The above-mentioned results strongly suggested the participation in the catalysis of the side chain of an amino acid having a pK_a value around 4.5. Thus, the chemical modification of the carboxylate side chains of antibody 13G10 was carried out by reacting this antibody with glycinamide in the presence of EDC. This modification caused a decrease in the peroxidase activity of 13G10-1 of about 50%. Since the same reaction, performed on the antibody which had been preincubated with hapten **1**, did not lead to any decrease in the peroxidase activity, it is likely that the observed loss of activity was due to the modification of a carboxylate residue located inside the binding pocket of 13G10.

4. Discussion

The association of a monoclonal antibody elicited against Fe(ToCPP) **1**, 13G10, and the corresponding Fe(ToCPP) co-factor has led to an artificial hemoprotein which is a remarkably thermostable catalyst for the peroxidase reaction. This complex is able to use not only H₂O₂ as oxidant but also a wide range of hydroperoxides such as alkyl, aralkyl and fatty acid hydroperoxides and catalyze their reduction 2–6-fold faster than Fe(ToCPP) alone does. Since H₂O₂ is the best oxidant when compared to bulky hydrophobic *tert*-butyl- and cumylhydroperoxide, it is likely that the Fe(ToCPP) co-factor is deeply inserted into its binding pocket in the antibody, with little space left over the plane of the porphyrin,

Table 2

Oxidation of ABTS by various hydroperoxides at pH 5, catalyzed by Fe(ToCPP) **1** and its complex with antibody 13G10^a

Catalyst	Rate of oxidation ^b (turnovers/min)			
	Oxidant: ROOH			
	R = H	R = Ethyl	R = <i>tert</i> -Butyl	R = Cumyl
1	0.85 ± 0.08	0.11 ± 0.01	0.61 ± 0.07	0.94 ± 0.11
13G10-1	4.72 ± 0.38	0.28 ± 0.03	2.09 ± 0.21	1.83 ± 0.18
13G10-1/ 1 ^c	5.7 ± 0.9	2.4 ± 0.5	3.4 ± 0.7	1.9 ± 0.4

^aFor experimental conditions see Section 2.

^bThe turnover numbers presented here are net values obtained after subtraction of the rates of oxidation observed for the reactions performed without catalyst, which ranged between 6.2 and 16 nM oxidized cosubstrate/min.

^cRate enhancement observed after complexation of **1** to antibody 13G10.

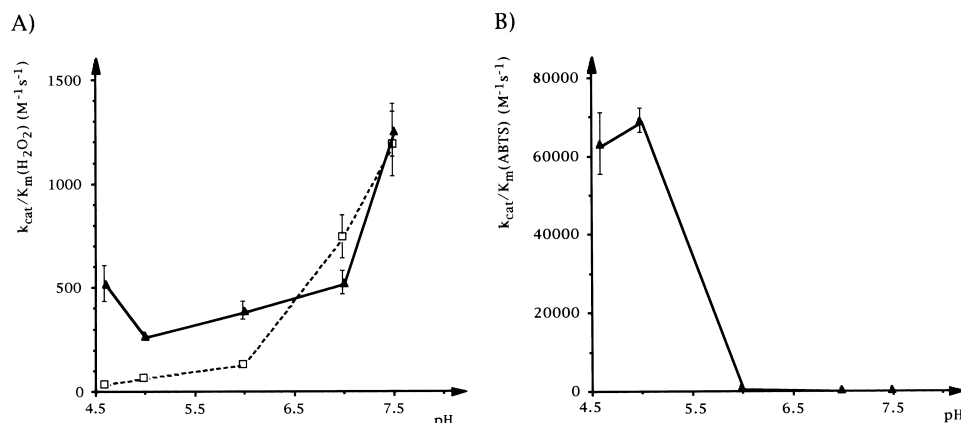


Fig. 5. pH dependence of the oxidation of ABTS (0.2 mM) by H₂O₂ (0.7 mM) in the presence of either **1** (□) or 13G10-1 (▲) as catalyst. A: Variations of $k_{\text{cat}}/K_m(\text{H}_2\text{O}_2)$ as a function of pH. B: Variations of $k_{\text{cat}}/K_m(\text{ABTS})$ as a function of pH. For experimental conditions see Section 2.

thus allowing the hydroperoxy group of the smaller molecule, H₂O₂, to interact with the iron atom. This is in agreement with our previous results on the comparison of the dissociation constants of various porphyrin-antibody complexes, amino acid sequences of L and H chains and chemical modifications of amino acid side chains of the antibody protein which showed that approximately two thirds of the porphyrin macrocycle were inserted inside the binding pocket of the antibody [30].

The 13G10-1 complex is also able to catalyze the oxidation by hydrogen peroxide of a variety of reducing cosubstrates such as ABTS, OPD, TMB and DMB 3–8-fold faster than **1** alone. The bicyclic aromatic ABTS and TMB were found to be the best reducing cosubstrates.

Kinetic studies have first shown that the oxidation of ABTS by H₂O₂ did not display saturation kinetics with respect to ABTS with **1** alone as catalyst whereas it did with 13G10-1 as catalyst. These results indicated that the interaction of 13G10-1 with ABTS was much higher than that of Fe(ToCPP) alone. At a constant concentration of ABTS, the reaction rates obtained for both catalysts showed saturation behavior against hydrogen peroxide, which is in agreement with a direct interaction of H₂O₂ with the iron atom of the porphyrin in both catalysts like in the case of peroxidases [27]. pH dependence studies have shown first that the K_m values for H₂O₂ varied similarly in the presence of either **1** or 13G10-1 as catalyst (Fig. 3), the lower $K_m(\text{H}_2\text{O}_2)$ values being found above pH 7. Although over the range of pH studied the $K_m(\text{H}_2\text{O}_2)$ value remained about 2–3 times higher for **1** than 13G10-1, the variations of the affinities of H₂O₂ for both **1** and 13G10-1 cannot be considered a determining factor to differentiate the two catalysts. In contrast, very different variations were observed for the k_{cat} values between pH 4.6 and 7.5 (Fig. 4) since with **1** as catalyst the k_{cat} value remained almost constant around 100 min⁻¹ whereas with 13G10-1 as catalyst it increased sharply below pH 5 to reach 540 min⁻¹ at pH 4.6. This phenomenon was thus at the origin of the larger rate enhancement and the sharp increase of the $k_{\text{cat}}/K_m(\text{ABTS})$ value observed at acidic pH with 13G10-1 as catalyst.

The above-mentioned results indicate that the catalysis of the peroxidase reaction by the 13G10-1 complex probably does not involve the participation of the side chain of an

amino acid such as histidine or arginine since k_{cat} does not vary significantly over pH 6 (Fig. 4). This is in agreement with our previous findings, based on selective chemical modifications of the amino acid side chains of the antibody protein [30], that probably neither histidines nor arginines participate in the catalysis although the latter residues are involved in the binding of the carboxylate substituents of **1** inside the antibody pocket. It is more likely that a residue with a side chain having a pK_a around 4.5, such as a carboxylic acid side chain, could participate, as a general acid base catalyst, to the heterolytic cleavage of the O–O bond of H₂O₂ to lead to the highly reactive iron(V)-oxo intermediate in the peroxidase mechanism. Accordingly, the modification of the carboxylic acid side chains of 13G10 by glycnamide caused a 50% decrease in the peroxidase activity of the 13G10-1 complex. In addition this proposal is in agreement with: (i) previously described results [36] which show that ammonium acetate is able to catalyze the heterolytic cleavage of the O–O bond of H₂O₂ in the presence of manganese porphyrins, (ii) the presence in the amino acid sequence of the complementary determining regions (CDRs) of the variable domain of 13G10 of amino acids with a carboxylic acid side chain such as glutamic acid, Glu-61 and Glu-99 respectively in the light chain CDR2 and CDR3, and aspartic acid, Asp-59 in the heavy chain CDR2. In this hypothesis, since k_{cat} is optimal at acidic pH, it is reasonable to think that the role of the carboxylic acid side chain would be to protonate the oxygen atom of H₂O₂ which is not bound to the iron atom of **1**. This would then facilitate the release of a water molecule in the medium, which would constitute the rate limiting step leading to the formation of the iron(V)-oxo species.

X-ray diffraction studies are currently under way to ascertain those results.

References

- [1] Lerner, R.A., Benkovic, S.J. and Schultz, P.G. (1991) *Science* 252, 659–667.
- [2] Benkovic, S.J. (1992) *Annu. Rev. Biochem.* 61, 29–54.
- [3] Thomas, N.R. (1994) *Appl. Biochem. Biotechnol.* 47, 345–372.
- [4] Schultz, P.G. and Lerner, R.A. (1995) *Science* 269, 1835–1842.
- [5] Thomas, N.R. (1996) *Nat. Prod. Res.* 13, 479–511.
- [6] Hsieh, L.C., Yonkovich, S., Kochersperger, L. and Schultz, P.G. (1993) *Science* 260, 337–339.

- [7] Hsieh, L.C., Stephans, J.C. and Schultz, P.G. (1994) *J. Am. Chem. Soc.* 116, 2167.
- [8] Shokat, K.M. (1988) *Angew. Chem. Int. Ed. Engl.* 27, 1172–1174.
- [9] Roberts, V.A., Iverson, B.L., Iverson, S.A., Benkovic, S.J., Lerner, R.A., Getzoff, E.D. and Tainer, J.A. (1990) *Proc. Natl. Acad. Sci. USA* 87, 6654–6658.
- [10] Wade, W.S., Koh, J.S., Han, N., Hoekstra, D.M. and Lerner, R.A. (1993) *J. Am. Chem. Soc.* 115, 4449–4456.
- [11] Wade, W.S., Ashley, J.A., Jahangiri, G.K., McElhaney, G., Janda, K.D. and Lerner, R.A. (1993) *J. Am. Chem. Soc.* 115, 4906–4907.
- [12] Crowder, M.W., Stewart, J.D., Roberts, V.A., Bender, C.J., Tevelrakh, E., Peisach, J., Getzoff, E.D., Gaffney, B.T. and Benkovic, S.J. (1995) *J. Am. Chem. Soc.* 117, 5627–5634.
- [13] Iverson, B.L. and Lerner, R.A. (1989) *Science* 243, 1184–1187.
- [14] Schwabacher, A.W., Weinhouse, M.I., Auditor, M.M. and Lerner, R.A. (1989) *J. Am. Chem. Soc.* 111, 2344–2346.
- [15] Cochran, A.G. and Schultz, P.G. (1990) *Science* 249, 781–783.
- [16] Cochran, A.G. and Schultz, P.G. (1990) *J. Am. Chem. Soc.* 112, 9414–9415.
- [17] Keinan, E., Sinha, S.C., Sinha-Bagchi, A., Benory, E., Ghazi, M.C., Eshhar, Z. and Green, B.S. (1990) *Pure Appl. Chem.* 62, 2013–2019.
- [18] Harada, A., Okamoto, K. and Kamachi, M. (1991) *Chem. Lett.* 953–956.
- [19] Keinan, E., Benory, E., Sinha, S.C., Sinha-Bagchi, A., Eren, D., Eshhar, Z. and Green, B.S. (1992) *Inorg. Chem.* 31, 5433–5438.
- [20] Savitsky, A.P., Demcheva, M.V., Mantrova, E.Y. and Ponomarev, G.V. (1994) *FEBS Lett.* 355, 314–316.
- [21] Savitsky, A.P., Nelen, M.I., Yatsmirsky, A.K., Demcheva, M.V., Ponomarev, G.V. and Sinikov, I.V. (1994) *Appl. Biochem. Biotechnol.* 47, 317–327.
- [22] Feng, Y., Liu, Z., Gao, G., Gao, S.J., Liu, X.Y. and Yang, T.S. (1995) *Ann. NY Acad. Sci.* 750, 271–276.
- [23] Takagi, M., Kohda, K., Hamuro, T., Horada, A., Yamaguchi, H., Kamachi, M. and Imanaka, T. (1995) *FEBS Lett.* 375, 273–276.
- [24] Kawamura-Konishi, Y., Hosomi, N., Neya, S., Sugano, S., Funasaki, N. and Suzuki, H. (1996) *J. Biochem.* 119, 857–862.
- [25] Kawamura-Konishi, Y., Neya, S., Funasaki, N. and Suzuki, H. (1996) *Biochem. Biophys. Res. Commun.* 225, 537–544.
- [26] Kohda, K., Kakehi, M., Ohtsuji, Y., Takagi, M. and Imanaka, T. (1997) *FEBS Lett.* 407, 280–284.
- [27] Marnett, L.J. and Kennedy, T.A. (1995) in: *Cytochrome P450: Structure, Mechanism and Biochemistry*, 2nd edn. (Ortiz de Montellano, P.R., Ed.), pp. 49–80, Plenum Press, New York.
- [28] Ortiz de Montellano, P.R. (1995), *Cytochrome P450: Structure, Mechanism and Biochemistry*, 2nd edn., Plenum Press, New York.
- [29] Quilez, R., de Lauzon, S., Desfosses, B., Mansuy, D. and Mahy, J.P. (1996) *FEBS Lett.* 395, 73–76.
- [30] de Lauzon, S., Quilez, R., Lion, L., Desfosses, B., Desfosses, B., Lee, I., Sari, M.A., Benkovic, S.J., Mansuy, D. and Mahy, J.P. (1998) *Eur. J. Biochem.* 257, 121–130.
- [31] Leondiadis, L. and Momenteau, M. (1989) *J. Org. Chem.* 54, 6135–6138.
- [32] Tsutsui, M., Ichikawa, M., Vohwinkel, F. and Suzuki, K. (1966) *J. Am. Chem. Soc.* 88, 854–855.
- [33] Köhler, G. and Milstein, C. (1975) *Nature* 256, 495–497.
- [34] De Lauzon, S., Desfosses, B., Moreau, M., Le Trang, N., Rajkowski, K. and Cittanova, N. (1990) *Hybridoma* 9, 481–491.
- [35] Hoare, D.G. and Koshland Jr., D.E. (1967) *J. Biol. Chem.* 242, 2447–2453.
- [36] Thellend, A., Battioni, P. and Mansuy, D. (1994) *J. Chem. Soc. Chem. Commun.* 1035–1036.